Pure appl. geophys. 157 (2000) 1707–1727
0033–4553/00/101707–21 $ 1.50 + 0.20/0

Pure and Applied Geophysics

Numerical Modelling of a Landslide-generated Tsunami: The 1979 Nice Event

S. Assier-Rzadkiewicz,[1] P. Heinrich,[1] P. C. Sabatier,[2] B. Savoye[3] and J. F. Bourillet[3]

Abstract—On the 16th of October 1979, a part of the Nice new harbour extension, close to the Nice international airport (French Riviera), slumped into the Mediterranean Sea during landfilling operations. A submarine slide with initial volume close to seashore of about 10 millions m^3, which could have evolved later into an avalanche, was followed by a small tsunami, noticed by several witnesses in the "Baie des Anges." The maximum tsunami effects were observed 10 km from the slide location near Antibes city, which was inundated. Previous analyses used rough approximate methods and produced models which did not conveniently fit data. In this paper, both the slide and the generated water waves are numerically simulated on the basis of the shallow water approximation. The landslide is assimilated to a heavy Newtonian homogeneous fluid downslope under gravity. Water waves are generated by sea-bottom displacements induced by the landslide. Taking into account a very accurate multibeam bathymetric map, the Nice slide of 10 millions m^3 is simulated by this model. The numerical results are generally consistent with the observed hydraulic local effects in front of the Nice airport, however they are not in agreement in the far field. A larger and deeper landslide 2 km off Nice airport is tested to quantitatively study the effects of the landslide volume on water waves generation.

Key words: Numerical modelling, fluid mechanics models, submarine flowslides, water waves, tsunami generation.

Introduction

Water waves resembling tsunamis and generated by a coastal underwater landslide can be as destructive as an earthquake-induced tsunami, when the involved volumes are sufficient (10^8 m^3) as well as the length scales (over a kilometre). This particular case of tsunamis, usually called "landslide-generated tsunami," is more localised than a classic tsunami and is characterised by shorter wave lengths and higher amplitude waves in the generation area. It can produce large run-up heights as the coast reaching several kilometres from the source.

[1] Laboratoire de Détection et de Géophysique, Commissariat à l'Energie Atomique, B.P. 12, 91680 Bruyères-le-Châtel, France.

[2] Laboratoire Physique Mathématique et Théorique, UPRES-A 5032, Université Montpellier II, 34095 Montpellier Cedex 05, France.

[3] Laboratoire Environnements Sédimentaires, Ifremer, Centre de Brest, DRO/GM, B.P. 70, 29280 Plouzané, France.

With the development of nearshore structures, risks associated with such hydraulic phenomena have increased. The most recent event occurred in November, 1994 in Alaska, where a submarine landslide killed a worker and significantly damaged Skagway harbour (KULIKOV *et al.*, 1996). The corresponding water waves were estimated by eyewitnesses to be 5–6 m in the inlet and up to 9–11 m at the shoreline. A second example is the landslide-generated tsunami that occurred off Nice on October 16th, 1979. A part of the building site of the new harbour slumped into the Mediterranean Sea (see photographs, Figs. 1a and 1b). Except for one person in Antibes, all victims were workers on the building site. The nearshore part of Antibes, located about 10 km from the building site on the opposite side of the Baie des Anges, was flooded with an estimated water elevation of 3 metres above sea-level. Although the initial slide was estimated around 10 millions m^3, the total volume ultimately surged probably to 150 millions m^3, which explains why two submarine cables (respectively located 75 km and 105 km from the triggering area and deeply beneath water), were broken 4h45 min and 9 h after the initial failure.

Within recent years several studies of the area were carried out by IFREMER (Institut Français de Recherche pour 1'Exploitation de la Mer), particularly SeaBeam surveys from which two bathymetric maps were produced: the "Carte Bathymetrique de la Baie des Anges Nice-Cote d'Azur" (PAUTOT, 1981) and the detailed bathymetric map of the source area (BOURILLET, 1991). Regional and local numerical Data Terrain Models were obtained respectively from these two maps by a geostatistical study. The Baie des Anges is located in the centre of the Ligurian continental margin. The top-continental shelf between 0 to 35 m water depth is narrow along the French Riviera and almost absent off Nice. The continental slope, beginning only a few hundred metres from the shoreline and severed by numerous canyons, is very steep with an average slope gradient greater than 10°. A depth of 1000 m is reached at only 5 km from the coastline. The sea-floor has been substantially modified by the 1979 event. The path of the 1979 event on the upper slope is marked in the present morphology by a steeply incised chute. The mass flow resulting from the initial landslide, triggered on a steep slope of about 10°, descended this thalweg that directly links the initial scar in front of the airport and the Var Canyon (dug by the Var River) at a water depth of about 1000 m. The flow was then channelled within the Var Canyon causing further erosion (MULDER *et al.*, 1997) and it turned into a turbidity current (PIPER and SAVOYE, 1993).

The Nice region is a region of high seismic activity with frequent earthquakes of magnitude greater than 4. This region also can be affected by distant earthquakes, with epicentres located mainly in the Ligurian Sea or in the continental part of the alpine chain. Associated with such distant earthquakes, three historical tsunamis affected the region of Antibes in 1564, in 1818 and in 1887 (HABIB, 1994). However, in the case of the 1979 event, the occurrence of an earthquake is completely discarded. No seismic event was recorded during or before this Nice event.

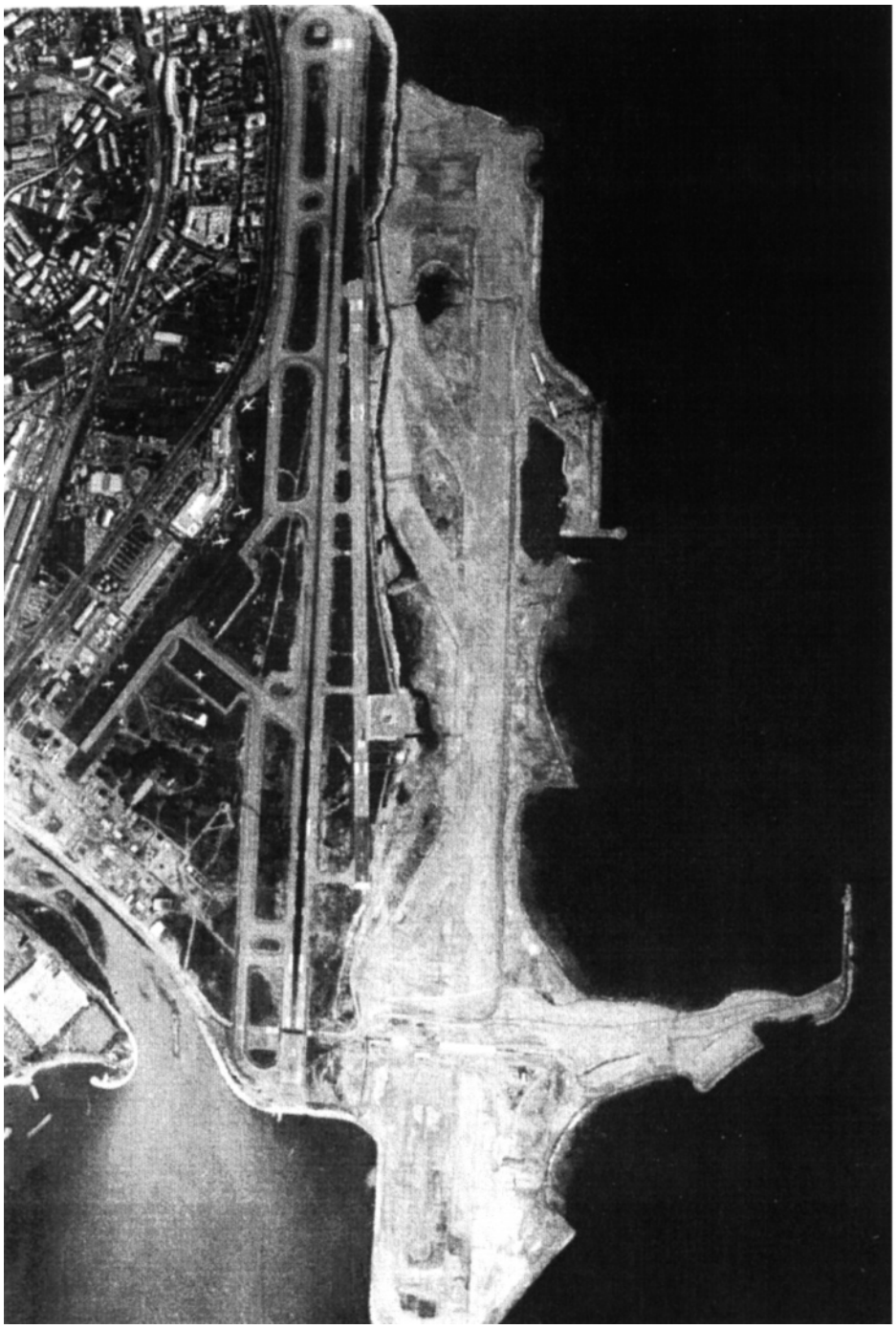

(a)

Fig. 1.

(b)

Figure 1
Photographs of the building site (a) before and (b) after the accident (PARIS-MATCH).

An accurate simulation of a slide tsunami involves modelling of the landslide and the generated water waves, considering the interaction of the slide body and water. To date, few numerical studies have taken into account this interaction. Most of them describe the landslide as one rigid body with a described motion (HEINRICH, 1992; HARBITZ and PEDERSEN, 1992). The landslide kinetic is imposed and the generation mechanism is simulated by making the water depth time-dependent (the fluid domain boundaries). Recently certain authors have modelled the interaction of the landslide with water, assuming that a submarine "flowslide" may be assimilated to the flow of a heavy viscous fluid. For instance, ASSIER *et al.* (1997), HEINRICH *et al.* (1998) have developed a 3-D model solving full Navier-Stokes equations for a mixture composed of water and a second heavier fluid. Their model is particularly appropriate to masses flowing down steep slopes, where vertical acceleration of the landslide and of water cannot be neglected compared to the gravitational acceleration. For gentle slopes and assuming large horizontal dimensions of the landslide compared to the thickness, the shallow water approximation may be used for both water waves and the landslide. Hence, FINE *et al.* (1999) have extended in 3-D the shallow water model developed by JIANG and LEBLOND (1992, 1993) that assimilates the landslide to a viscous flow and deals with the interaction between water waves and the landslide, both modelled on the basis of the shallow water assumption. From a computational perspective the latter models do not allow for vertical space variables and may be used considerably easier than full Navier-Stokes models. Due to the high computational cost of 3-D Navier-Stokes simulations for actual events, a shallow water model has been developed similar to FINE *et al.* (1999) and is presented in this paper. Water wave heights are overestimated by shallow water models compared to Navier-Stokes models at two stages of the simulation. First, during the generation phase, the water surface deformation is assumed to be identical to the bottom deformation, as is explained in the Appendix (remark 2). Second, frequency dispersion affecting the propagation of water waves is not taken into account.

Fixing Facts and Chronology of Events

Because of casualties and the observed slide, a committee (MIP) had to gather observations, organize them into ordered events, and suggest explanatory models. The MIP (MIP, 1981) gathered observations, proposed a chronological sequence of events, and analysed the effects of a 8 millions m^3 slide with a reasonable range of velocities. They concluded that they had no evidence of events which may have triggered this slide and not enough evidence of its extensions in deep water, but that the slide itself and its hydraulic consequences are sufficient to explain casualties at the airport and are partly consistent with the accident in Antibes-La-Salis. Hence the next question is rather that of the dam stability, and the MIP hydraulic studies

could be closed. However, both at that time and later, some authors disagreed with the MIP model emphasis of the observed slide. They pinpointed that this simplest model does not fit all "data," and attempted to improve it. It is clear that the consistency of several models with "data" is made easy in this problem by the lack of true measurements (two tide gauges give figures, however their time constant is much larger than wave periods), and by the sparseness and discrepancies in time or amplitude evaluations by witnesses, which never notice the effect from its very beginning. Bathymetry and submarine observations are also available, although of course information they supply needs a thorough analysis.

So as to produce a terse survey of models, we first give the most likely comprehensive chronological sequence of "reported" events at various locations, with estimated times. We shall then go through the previous models, which differ by assumptions on causes and fits of "data." In the chronology given below of the (beginning of) events, the coordinates of witnesses "observations" are shown (see Fig. 2) as:

Ai = New Nice harbour works, close to the Airport control tower (where the best observations were made).

PC = "Port de clapage" (a small harbour for special works located at 1 km northeast of Ai).

AS = Shore of Antibes-La Salis.

Harbours are labelled as *Ni* (Nice), *Vi* (Villefranche), *SL* (Saint Laurent du Var), *PV* (Port-Vauban, Antibes). *Ni* and *Vi* are respectively, 8 km and 10 km east of *Ai*

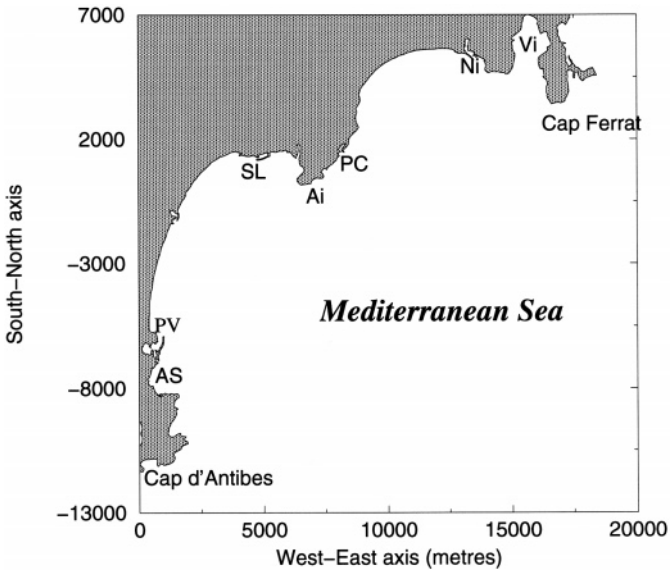

Figure 2
Simplified regional map of the "Baie des Anges."

location. *SL* is 2 km west of *Ai* location. Other locations are put explicitly. Time "zero" is defined as $t_0 = 13\text{h}57$.

Main Chronology

Before "time zero," the following information was given, but was dubious due to discrepancies of different witnesses:
10h30, 11h30, *Ni*—unexpected water waves with amplitudes of 0.3 to 0.6 m.
$\sim$ 13h40, *Vi*—unexpected lateral impulses on boats.
13h55–13h56, may be some of the events recorded below begin.

$$t_0 = 13\text{h}57$$

Ai. Dam and embankments ($+9$ workers and tools) slide into sea and disappear offshore: motion extending from centre to east and west, no longer apparent outside after 14h02. Local waves were observed.

On the seismogram of Nice, the usual "noise" increases: the increase lasts, with variations, from perhaps 13h55 up to 14h15–14h20, with maxima between 14h04 and 14h09.

$$t_0 \leq t_1 \leq t_0 + 1 \text{ min}$$

SL. Damped oscillation (period ~ 3 min, beginning with trough ≥ 2 m, then crests or troughs ≤ 1 m, up to 14h50).

$$t_2 \sim 14\text{h}02 = t_0 + 4 \text{ min}$$

PC. Damped oscillations (period ~ 7 min, beginning with a crest of 2 to 3 m).
Ni. Damped oscillations (period ~ 8 min, beginning with a crest of about 1.2 m).

$$t_3 \sim 14\text{h}06 = t_0 + 8 \text{ min}$$

AS. Three oscillations (almost equal size, 2.5 m to 3.5 m, period ~ 9 min) beginning with a crest at t_3. A forerunner had been observed by one witness around 14 h: 0.5 m crest followed by a smaller trough. Last motions around 14h30.
PV. Similar observations but time shift of (-1 min) and amplitudes about three times smaller.

$$t_4 \sim 14\text{h}08 = t_0 + 10 \text{ min}$$

Vi. Damped oscillations (period ~ 8 min) beginning with a crest of about 1.8 m.

$$t_5 \sim 14\text{h}13 = t_0 + 15 \text{ min}$$

In the harbour of Cannes located outside of Figure 2, 25 km southwest of *Ai*, damped oscillations are observed (amplitudes ≤ 1 m, period > 15 min).

Previous Studies

Several harbours contained a tide-gage whose inertial effects average surface motions over several minutes, filtering off oscillations of smaller period. Those of Nice and Villefranche show that the average sea level probably declined during the first 12 minutes, beginning respectively around $t_0 + 3$ min and $t_0 + 6$ min, some 10 cm at *Ni* and 5 cm at *Vi*, then recovered completely after 2 h. However these figures have broad error margins. Additional information (oscillation periods of 8 to 10 min) corresponds to resonance modes in the Nice harbour and in the bay of Villefranche.

At 18h45 and 22h50, two cables were cut under deep water distant from *Ai* (75 km and 105 km), presumably by turbidity currents whose average speed is hence estimated at 17 km/h during the five first hours, 7 km/h in the four following hours.

Later soundings were taken, partly by submarines, and compared to the bathymetric measurements previously available. They indicated that the observed slide near *Ai* not only involved sediments deriving from human activity but also sediments stripped from the slope. The part above 150 m depth corresponds to 10 millions m^3 or so. They went down a "channel" 450 m wide which yields at deepest depth two canyons (east and west) eventually joining that of Var River (Var Canyon) at a depth around 1000 m. Slopes near *Ai* had recovered their natural stability figure ($\sim 20\%$).

Several submarine observations confirmed that ground stripping was superficial near *Ai* and that sediments had flowed West Canyon. They displayed certain evidence of a turbidity flow probably initiated by avalanche effects at substantial depth in Var Canyon. However they produced neither evidence of slides arising from Var River or evidence of slides on canyon flanks or of other recent large slides beyond the range of the *Ai* slide.

Proposed Models in the Past

In the early eighties, two classes of models were produced, each class containing a "simple model" and improved ones. Keeping in mind the observations, "strong" and "weak" points of models were analysed on the basis of ray-tracing methods and analytical methods, such as the one described in the appendix.

Models of the First Class

(1) In the "simple" one, suggested by MIP, they attempt to derive all the observed events from the only slide for which there is strong evidence, that close to *Ai*. They describe it as a whole body of 8×10^6 m^3, sliding with reasonable velocities (40 km/h at 150 m depth, which is consistent with that of the subsequent turbidity current).

"Strong" points: Ray-tracing methods show that it fits many arrival times, up to uncertainties and nearby amplitudes.

"Weak" points: (a) Some arrivals around $t_0 + 4$ min may correspond to fairly different travels from *Ai*, and witnesses provided evidence for early arrivals at time $t_0 - 1$ min. In particular, *SL* seems to "begin" too early. (b) Even if the model is recalibrated and predicts excessively large amplitudes in *PC*, they are much too small in *AS*, where such a simple source is unlikely to excite the observed resonance.

(2) Improvements to this model were proposed by HABIB (1994), who assumes that an initial release of some 4×10^6 m^3 of sediments began around 13h54 on the slope of Var delta (a few km west of *Ai* location). This release induced at deeper depth a regressing slide to location *Ai*, whose upper part is concerned at 13h57. The arrival time in *SL* is therefore explained, *PC* is in the dam shadow before 13h58, the source disymmetry and time signature favour resonances, there is no strong inconsistency with submarine observations which were not accurate in the upper range, and one obtains a better explanation of the seismic noise increase.

In all these models of the "first class," it is understood that after the slide submerged beyond a depth of approximately 200 m, it gradually increased (up to 1 to 2×10^8 m^3) by erosion and perhaps avalanches, and eventually produced the turbidity current that destroyed the two cables.

Model of the Second Class

As a matter of fact, the idea of D.D.E. (Direction Départementale de l'Equipment, 1981) joined that of BOLTON SEED (1983), so that we can describe it as one model, with small variants. This model differs from the MIP model by introducing the assumption of a massive slide (around 10^8 m^3 in Seed, more in DDE), beginning around 13h54, and located on the flanks of Var Canyon some 15 km to 18 km off Nice (depth ≥ 1500 m). This slide presumably explains most hydraulic effects and the quasi-tidal effects produced at the location *Ai*, or another coupling mechanism supposedly induces the *Ai* slide.

"Strong" points: it explains that large phenomena of the same order and fairly simultaneous (around t_3) were observed at several locations remote from each other. It may explain the seismic noise level from 13h54, however the orders agree only if the slide is disconnected into several successive ones.

"Weak" points: it is assumed that the generation range would be 5×2 km^2, 15 km from the coast, and this distance supports arguments of the preceding "strong point." However, if we blindly follow it, and if we observe that several waves were sighted, each one with a period around 500 s, such that the length of a given sign deformation is deca-kilometric, and that this model presumably shows that the above phenomenon extends at given time $\sim t_3$ on at least 30 km of shoreline, if we add the hydraulic consequences of chopping the source, whose velocity can hardly

exceed 20 km/h, we see that several times 10^8 m^3 are necessary to fit all amplitudes according to the analytical formula (see Appendix), and that other evidence should support this guess.

Whatever the models, ray-tracing methods and analytical methods cannot accurately describe the resulting hydraulic phenomena, such as trapped waves along the coast or the focusing of waves. It is proposed to use recent numerical methods to confirm or infirm the proposed hypothesis.

Description of the Numerical Model

Two numerical models, based on the shallow water approximation, have been developed, one for the tsunami propagation, the other for the landslide considered as the flow of a viscous fluid. This implies that the characteristic wavelengths are considerably larger than the water depth and that the slide thickness is much smaller than the characteristic slide length. For both media, depth-averaging over the water depth or over the slide thickness is performed, assuming hydrostatic pressure. The sea-bottom deformation induced by the landslide is used as input data in the tsunami model.

Tsunami model

Depth-averaging the equations of mass and momentum conservation leads to evolution equations for h, $(h\,.\,u)$ and $(h\,.\,v)$, where h is the water layer thickness and $\boldsymbol{u} = (u, v)$ is the depth-averaged horizontal velocity. In a conservative form, these equations read:

$$\frac{\partial h}{\partial t} + \frac{\partial}{\partial x}(hu) + \frac{\partial}{\partial y}(hv) = 0 \tag{1}$$

(mass conservation equation)

$$\frac{\partial}{\partial t}(hu) + \frac{\partial}{\partial x}(hu.u) + \frac{\partial}{\partial y}(hu.v) = -\frac{1}{2}\frac{\partial}{\partial x}(gh^2) + gh\frac{\partial d}{\partial x} \tag{2}$$

$$\frac{\partial}{\partial t}(hv) + \frac{\partial}{\partial x}(hv.u) + \frac{\partial}{\partial y}(hv.v) = -\frac{1}{2}\frac{\partial}{\partial y}(gh^2) + gh\frac{\partial d}{\partial y} \tag{3}$$

(momentum conservation equations)

where $d(x, y, t)$ is the bathymetry and is related to h by $h(x, y, t) = d(x, y, t) + \eta(x, y, t)$, $\eta(x, y, t)$ being the water surface elevation. Temporal variations of d induced by the landslide are taken into account in the mass conservation equation.

Landslide model

In this study, the mechanism initiating the landslide is not studied and it is assumed that the whole mass suddenly loses its equilibrium. For simplicity, the landslide is considered as a viscous fluid (NOREM *et al.*, 1991; FINE *et al.*, 1999)

flowing down the slope under gravity forces without dilution, erosion and deposition. Mass and momentum conservation equations are depth-averaged over the slide thickness similar to tsunami equations, which allows the precise mechanical behaviour within the flow to be ignored. Equations are written in a coordinate system linked to the topography. In this system, (x, y) and z denote respectively slope parallel and slope normal coordinates, $h(x, y, t)$ is the layer thickness perpendicular to the slope and the velocity $\boldsymbol{u} = (u, v)$ is the depth-averaged velocity parallel to the bed (HUTTER, 1996). The interface between water and mass is assumed to be stress-free, while longitudinal gradients of the deviatoric stress are neglected throughout the flow. The continuity equation (1) is unchanged and the momentum equations read:

$$\frac{\partial}{\partial t}(hu) + \alpha \frac{\partial}{\partial x}(hu.u) + \alpha \frac{\partial}{\partial y}(hu.v) = -\frac{1}{2}\kappa \frac{\partial}{\partial x}(gh^2 \cos\theta) + \kappa gh \sin\theta_x - \tau_{xz(z=0)} \tag{4}$$

$$\frac{\partial}{\partial t}(hv) + \alpha \frac{\partial}{\partial x}(hv.u) + \alpha \frac{\partial}{\partial y}(hu.v) = -\frac{1}{2}\kappa \frac{\partial}{\partial y}(gh^2 \cos\theta) + \kappa gh \sin\theta_y - \tau_{yz(z=0)} \tag{5}$$

$$\kappa = 1 - \rho_w/\rho_s \tag{6}$$

where ρ_w and ρ_s are the water and sediments densities, with a density ratio $\rho_s/\rho_w = 2$, $\tau_{xz(z=0)}$ and $\tau_{yz(z=0)}$ are the shear stresses at the bed surface, $\theta(x, y)$ is the local steepest slope angle, θ_x and θ_y are the slope angles along x- and y-axis, respectively. The viscous flow is associated with a parabolic profile of the horizontal velocity, with a no-slip condition at the sea-bottom (JIANG and LEBLOND, 1992). In this case, $\alpha = 6/5$ and the shear stress at the sea-bottom reads:

$$\tau_{xz(z=0)} = -3\mu u/(h\rho_s) \tag{7}$$

where μ is the dynamic viscosity.

It is worth noting that equations of tsunami propagation are similar to those governing the landslide, when written in a conservative form. Both systems (1, 2, 3) and (1, 4, 5) are composed of nonlinear hyperbolic equations and are solved by means of a common finite-difference method on the same staggered grid. The numerical model is based on a shock-capturing method, and uses a Godunov-type scheme, extended to the second order (MANGENEY *et al.*, 2000). It is particularly adapted to strongly propagate nonlinear waves in the tsunami model or to reproduce steep fronts in the landslide model.

The computational domain extends over 14.5 km in the west–east direction and 22.5 km in the south–north direction, with a grid step of 50 metres. In our study, coastal inundation is not calculated by the tsunami model, since irregularities of the topography cannot be modelled by the grid step of 50 m. The computation is stopped at the flow depth on the shoreline, the latter being taken as a perfect

reflector. Our model, referred to in the literature as a threshold-type model, uses a minimum depth contour of 5 metres.

Numerical Modelling of the Nice Event

Simple "First Class" Model

The slump of the building site (corresponding to the simple "first class" model) is simulated assuming that the mass liquefies instantaneously and behaves as a viscous fluid while sliding downslope. Figures 3a and 3b present the local bathymetry map of *Ai* before and after the October 16th, 1979 accident off Nice. By difference of these two maps, an initial volume of 8.7 millions of m^3 has been calculated. The sediments are 0 to 50 metres thick, covering an area of approxi-

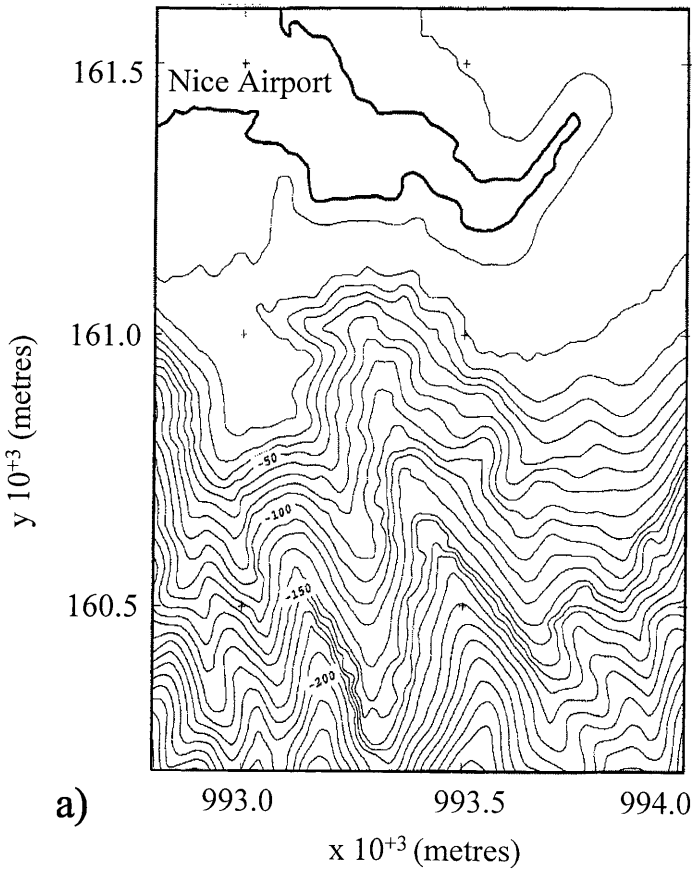

Fig. 3.

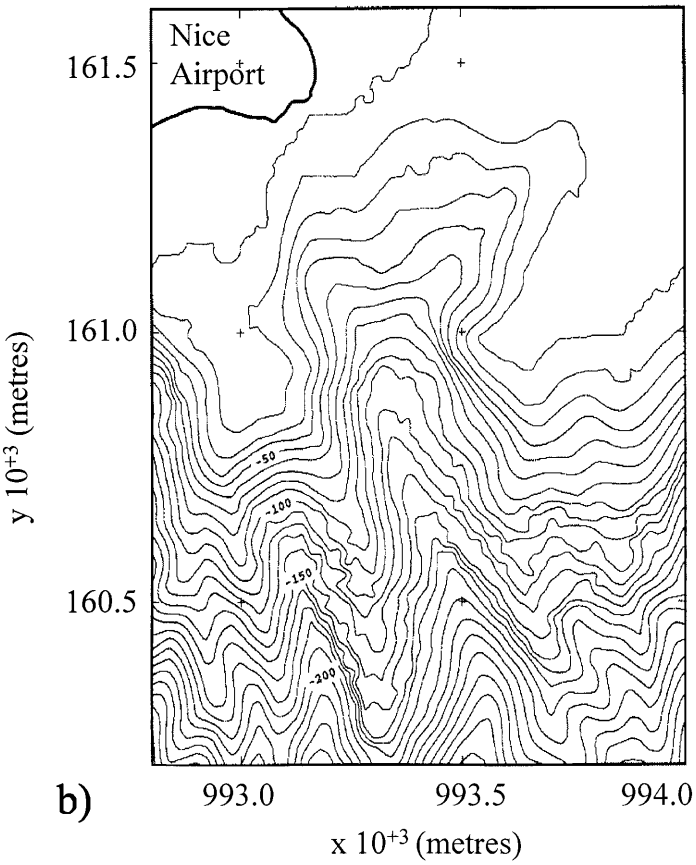

Figure 3
a) Local bathymetric map of the source area of the 1979 Nice event before the landslide. b) same as a), after the landslide. This map is interpolated on a mesh used in the numerical simulation. The landslide is defined by the difference between the two maps a) and b).

mately 700 m by 900 m. The 3-D geometry of the slide and the bathymetry are shown in Figure 4. The aim of this first simulation is to determine the possibility of reproducing the observed tsunami in the entire computed domain.

The influence of the viscosity on water waves generation is investigated by varying, for the same geometry, the kinematic viscosity from 0.25 to 25 m^2s^{-1}. The resulting mean velocities of the landslide reach 4 m/s to 10 m/s between 25 and 50 s after the landslide initiation and then decrease very slowly. It is shown that for small viscosities lower than 1 m^2s^{-1}, the whole landslide is not guided in the main channel and an important part slides eastward, which does not match the observations. The computed mud flows are shown for $v = 2.5$ m^2s^{-1} in Figure 4 at different times after the landslide beginning. At $t = 120$ s, the front of the mud has flowed about 2 km into the thalweg. At $t = 240$ s, the flow is separated into three parts in

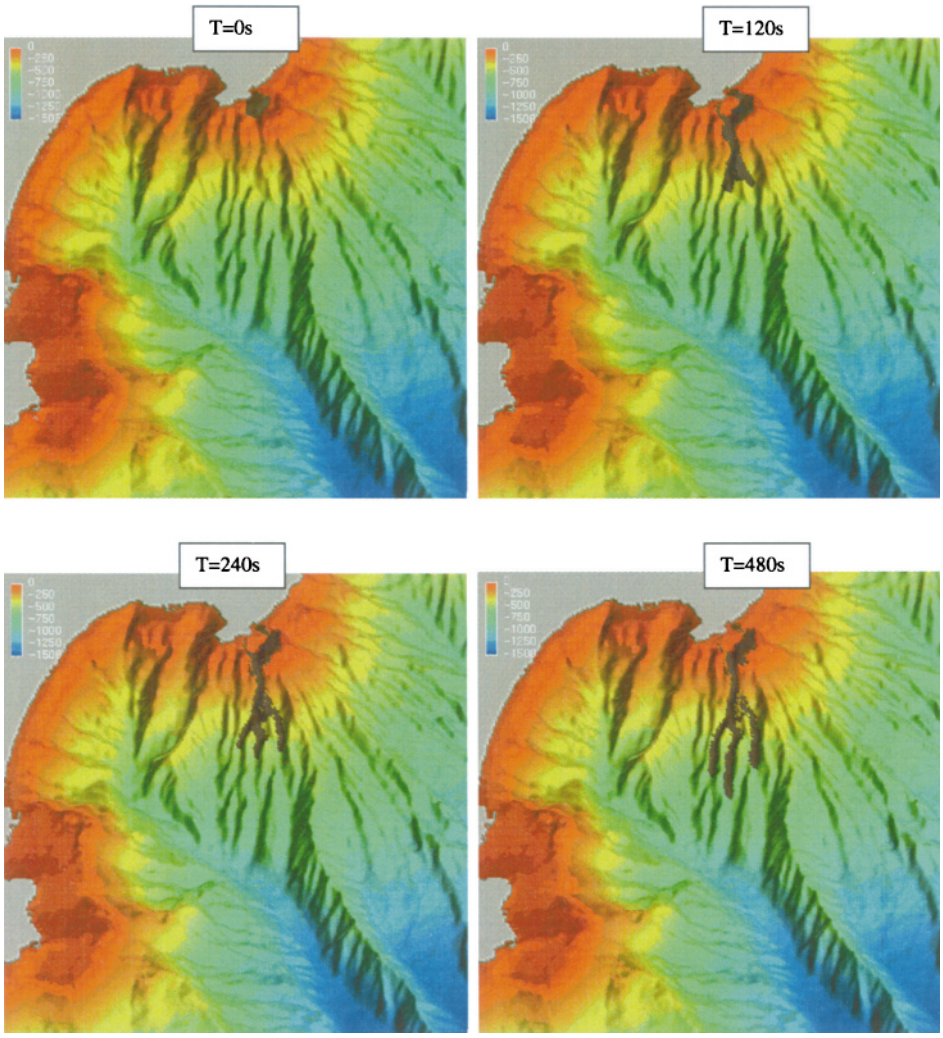

Figure 4
Three-dimensional view of the bathymetry and of the landslide represented in black. The slump of the building site, with a volume of 8.7 millions of m^3, is assimilated to a viscous flow with $v = 2.5\ m^2 s^{-1}$. The vertical scale has been exaggerated by a factor of 4.

three different channels. Numerical tests show that the perturbation of the water surface by the landslide is negligible after T = 120 seconds. The associated computed water surfaces are represented in Figure 5 at T = 60 s and T = 120 s. At the source location, the water ahead of the front face of the slide is pushed away, creating a leading positive wave in the slide direction, with a maximum amplitude of about 2 metres. The second wave is a large trough simultaneously created by the slide aspiration trough, with a maximum of 10 metres. The two waves spread outward

from the source as cylindrical waves. At T = 60 s, the dam has disappeared into the sea and a positive wave of about 2 m reaches *PC*, located at about 1 km northeast of *Ai* location (Fig. 5). This amplitude fits the observed data, although the arrival time is shorter than the observed one, which could be due to the hypothesis of an instantaneous landslide in the model. At T = 120 s, the numerical results reveal that a positive wave propagates into the east (toward *Ni* and *Vi*) and west directions (toward *SL*), contrary to the tide-gage records and the observations. In the slide direction, i.e., toward *AS*, the positive wave travels at a phase velocity close to $(gh)^{1/2}$ and its height decreases rapidly due to geometric dispersion and increasing depth.

Comparisons of water at Antibes and Nice airport for different viscosities (Fig. 6) show that this parameter has little or no influence on periods and reduces only slightly wave amplitudes. Similar conclusions are found by FINE *et al.* (1999) and by JIANG and LEBLOND (1992) for kinematic viscosities ranging from 0.01 to 2 $m^2 s^{-1}$. Wave periods at both sites range from 1 to 2 minutes, which does not fit observations. The gage at the airport is located on the artificial dyke, 4 metres above sea-level (Fig. 6). As the dam disappeared into the sea, a large trough is formed with a maximum of about 10 metres, 30 seconds after the start of the landslide, and could have caused the death of nine workers. It is followed by a positive wave created by the filling-in of the trough with amplitudes ranging from 2.5 to 3.5 metres, which is probably responsible for the airport inundation. At Antibes, water wave heights do not exceed 1.5 metres above sea-level, which is probably not sufficient to inundate Antibes. Moreover, it is worth noting that these heights are overestimated due to the absence of frequency dispersion from *Ai* to

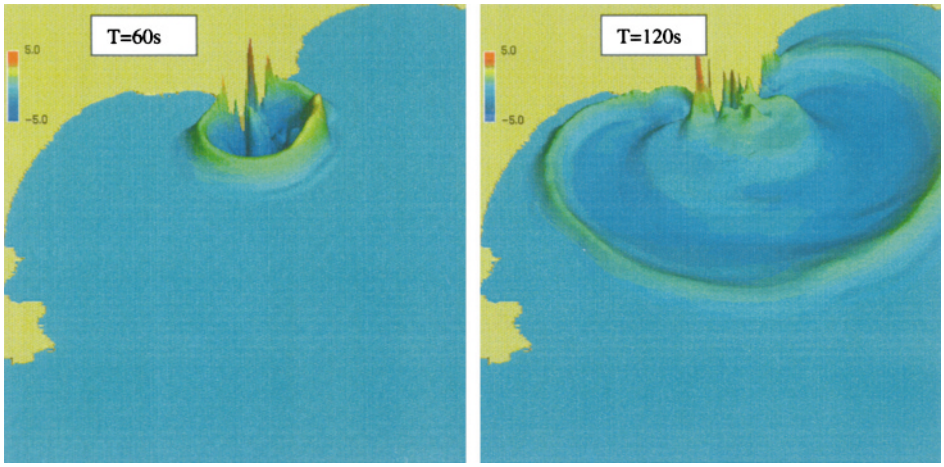

Figure 5
Snapshots of the associated water surfaces calculated at T = 60 s and T = 120 s after the landslide initiation. Vertical scale is exaggerated by a factor 500 with respect to the horizontal dimensions.

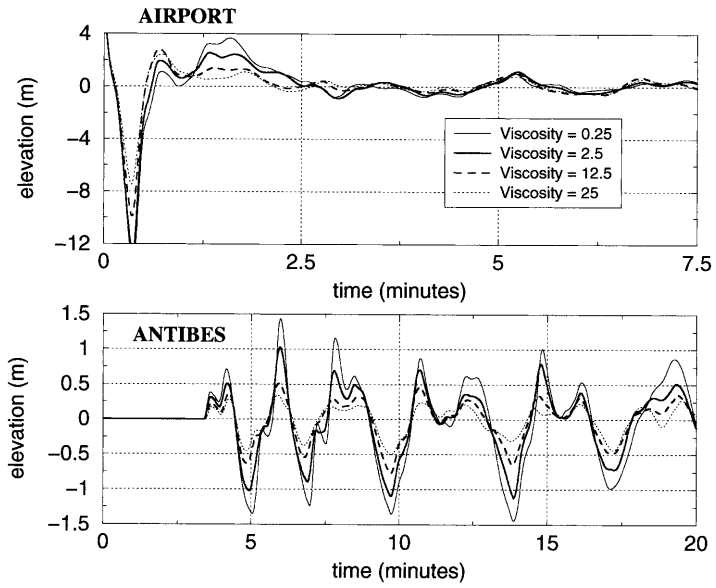

Figure 6
Influence of the viscosity on water waves generation for values varying from $v = 0.25$ m^2s^{-1} to $v = 25$ m^2s^{-1}. Water wave heights are compared at the building site and in front of Antibes harbour (*PV*).

Antibes, and due to the perfect reflection at the Antibes shoreline. The main results of this simulation illustrate that the observed hydraulic local effects in front of *Ai* are approximately reproduced by the model. However, two negative results relative to the "first class" model must be pointed out. First, the energy of the first wave propagating southwest is not sufficient to inundate Antibes. Second, the first wave observed at *SL* and recorded by tide-gages (*Ni* and *Vi*), is negative, which is not reproduced by the simulation. This discrepancy suggests that the 1979 observed tsunami was probably not generated only by 10 millions of m^3 landslide off Nice.

Improved "First Class" Model

One means of reproducing the tsunami is to select the sites with steep slopes, where a submarine landslide of several tens of millions of m^3 could have occurred, and to carry out the associated simulations. Since the number of these sites is large, we rather propose in this paper to study the hydraulic effects of one deeper and larger landslide, corresponding to an improved "first class" model. Models of the "second class" located at water depths greater than 1500 metres are not envisaged. To reproduce water wave heights of 2 to 3 metres, such models require volumes of several hundreds of millions of m^3, for which evidence was not found. Arbitrarily, a landslide with a volume of 70 millions of m^3 has been chosen, located at the bottom of a canyon 3 kilometres southwest off *Ai* (Fig. 7). The landslide area is 2

km by 1 km with a maximum thickness of 150 metres, at water depths ranging from 400 m to 650 m. For the same range of viscosities, the resulting mean velocities of the landslide are larger and reach 8 m/s to 18 m/s between 25 and 50 seconds after the landslide initiation. Figure 7 shows the computed mud flows at T = 0, 120, 240 and 480 seconds for a kinematic viscosity of $\nu = 2.5$ $m^2 s^{-1}$. Figure 8 displays the 3-D view of the associated water waves. The same hydraulic phenomena are

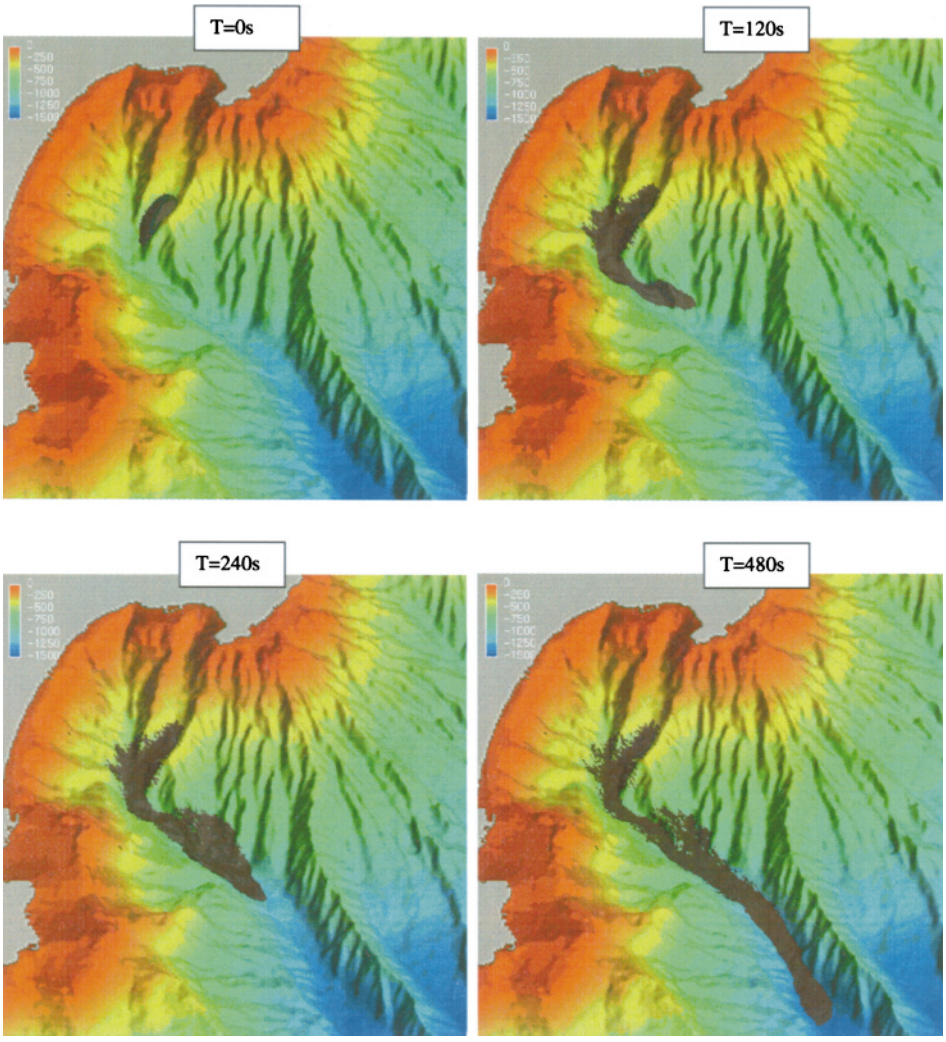

Figure 7
Simulation of a landslide with a volume of 70 millions of m^3, assimilated to a viscous flow with $\nu = 0.25$ $m^2 s^{-1}$. The landslide volume is defined as the intersection of an ellipsoidal volume with the existing bathymetry and covers approximately an area of 2 km by 1 km, with a maximum thickness of 150 metres.

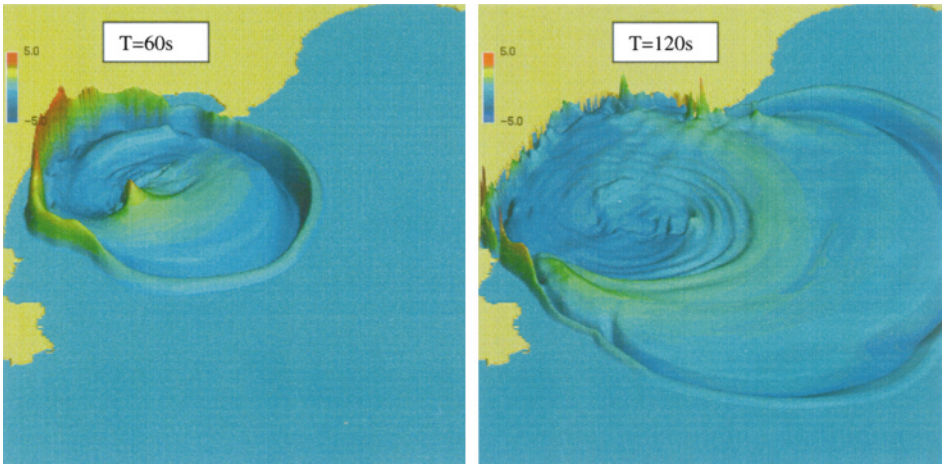

Figure 8
Snapshots of the associated water surfaces calculated at T = 60 s and T = 120 s after the landslide initiation. Same 3-D view as in Figure 5.

obtained at the source location: the formation of a positive wave and a large trough, followed by a second positive wave.

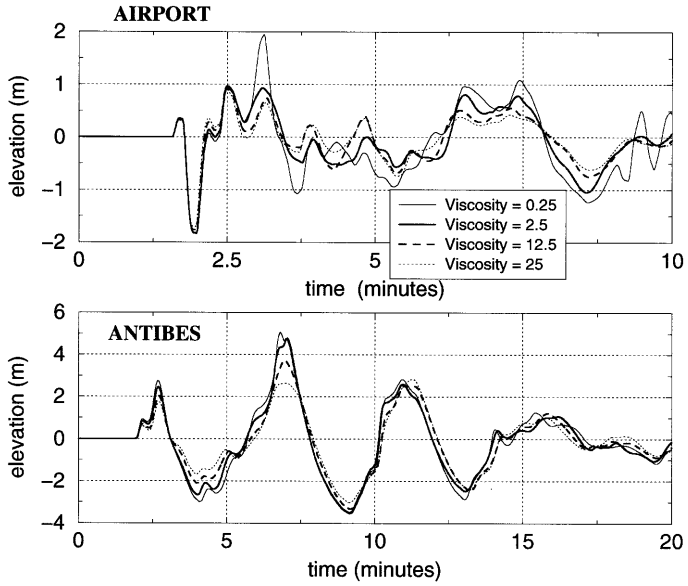

Figure 9
Comparisons of water wave heights at the building site and in front of Antibes harbour (*PV*) for kinematic viscosities ranging from $\nu = 0.25\ m^2s^{-1}$ to $\nu = 0.25\ m^2s^{-1}$.

Water waves are compared in Figure 9 at Antibes and Nice for viscosities ranging from 0.25 to 25 m^2s^{-1}. Wave periods approach 4 minutes, 2 times longer than those observed for the former landslide although 2 times shorter than those observed in *AS*. At Antibes, maximum water wave heights are larger by at least a factor of 3 than those generated by the small landslide, which better matches the observations. In the Nice region, an imperceptible positive wave (probably disappearing if frequency dispersion is provided for) precedes a trough of 2 metres high, in better agreement with the description of witnesses and with the first movement recorded by tide gauges.

Although arbitrarily located, such a landslide, occurring approximately at the same time as the slump of the building site, could account for the first negative movement observed at *Ni*, *Vi* tide gauges and *SL* location. Moreover, the amplitudes and the periods in the *AS* region better match the observations. However, the chronology is still not reproduced, neither in *AS*, nor in the Nice region.

Conclusion

This paper presents a numerical model simulating the sliding of a mass along a slope and the propagation of the associated water waves. This model has been applied to the simulation of the slide tsunami off Nice in 1979.

Numerical results indicate that the inundation observed in front of the airport could be created by an underwater landslide of about 10 millions of m^3. However, taking into account the witnesses' observations in the Baie des Anges and the negative wave recorded by tide gages, it is concluded that this landslide is not sufficient to reproduce the entire observed tsunami.

The total involved volume of the 1979 slide has been estimated at about 150 millions of m^3. The preliminary results of simulations of a larger and deeper landslide better match some of the observations, which does not mean however that the selected landslide could be responsible for the observed tsunami. The results of the two simulations suggest only that such a scenario probably occurred, approximately at the same time as the sliding of the building site.

Appendix

Before surveying models, the reader interested in hydraulic effects should remember very simple approximate results (see for instance SABATIER, 1986) that hold for small perturbations, in the case of a coast roughly invariant by translation (y coordinate axis), the horizontal axis x being oriented towards

deep water, and $z = 0$ being the zero sea level and the depth being a smooth function $h(x)$ of x only (or almost only). With this geometry, that which we cell A is the "area" of a deformation but in three dimensions it would mean its volume.

(1) A sharply localised (at $x = x_0$) and sudden (at $t = 0$) bottom deformation ($z = -h(x_0) = -h_0$) of "area" A yields at $z = 0$, at time $t = 0^+$, an initial surface deformation η of area A but whose maximum amplitude decreases with depth, and whose width increases accordingly, the shape being very smooth:

$$\eta \approx A\left[2h_0 \cosh \pi \frac{x - x_0}{2h_0}\right]^{-1}.$$

(2) A sudden bottom deformation at $t = 0$ whose range is very comparative to average depth (which corresponds to the shallow water hypothesis) yields at $t = 0^+$ an initial surface deformation of equal area and whose shape is roughly identical to that of the bottom deformation.

Both in cases (1) and (2), the initial surface deformation propagates as t increases, leading first to one wave then several because of dispersion and the largest amplitude decreases with distance r at least as $r^{-1/2}$ along the coast and as r^{-1} in deep water, unless special bottom configurations trap the energy. The local signal velocity is of the order of $c = (gh)^{1/2}$.

(3) Using the remarks (1) and (2), we can model a slow slide by a couple of positive (P) and negative (N) bottom deformations averaging to zero area respectively at the beginning and end of the slide, and propagating at velocity v (so that A is a function of $(x - vt)$). It is clear that if v is smaller than the group velocity c, the negative waves they induce at sea surface negatively interfere and the resulting amplitude η is reduced. In the conditions of remark (2) an approximate result is that η travels with local signal velocity although its amplitude is reduced by a factor averaging (over the generation range) the Froude number v/c.

Since P is positive, the surface wave it induces is positive, but its amplitude is smaller than that produced by N because of the depth factor (P is located further offshore), and it propagates faster. Hence the first signal should typically exhibit a small positive forerunner followed by a large trough, and it is only distant from the source (or if resonances are excited) that a set of nearly equal period waves can show.

Acknowledgements

The authors are grateful to IFREMER for providing bathymetric data and to Dr. J. Bouchez who made possible the collaboration between the different institutes.

REFERENCES

ASSIER, S., MARIOTTI, C., and HEINRICH, PH. (1997), *Numerical Simulation of Submarine Landslides and their Hydraulic Effects*, J. Waterway, Port, Coastal, and Ocean Engin. *123*, 149–157.

BOLTON SEED, H. (1983), *Réchêche de la cause du glissement du Port de Nice*, *survenu le 16/10/79* (unpublished report).

BOURILLET, J. F. (1991), *Géomorphologie à partir d'un Modèle Numérique de Terrain (Baie des Anges)*, 3e Congrès Français de Sédimentologie, Livre des Résumés, Publications ASF, Paris *15*, 51–52.

DDE (1981), *Rapport de la Direction Départementale de l'Equipement des Alpes-Maritimes du 17 juillet 1981 sur le sinistre du 16/10/79* (unpublished report).

FINE, I., RABINOVICH, A., KULIKOV, E., THOMSON, R., and B. BORNHOLD (1999), *Numerical modelling of landslide-generated tsunamis with application to the Skagway harbor tsunami of November 3, 1994*, International Conference on Tsunamis, Paris, France, May 26–28, 1998, Publications CEA-LDG, BP12, 91680 Bruyeres-le-Chatel, France, 211–223.

HABIB, P. (1994), *Aspects géotechniques de l'accident du nouveau port de Nice*, Revue Française de Géotechnique *65*, 2–15.

HARBITZ, C., and PEDERSEN, G. (1992), *Model Theory and Analytical Solutions for Large Water Waves due to Landslides*, Preprint series, Dept. of Mathematics, University of Oslo, no. 4.

HEINRICH, P. (1992), *Nonlinear Water Waves Generated by Submarine and Aerial Landslides*, J. Waterway, Port, Coastal, and Ocean Engin. *118* (3), 249–266.

HEINRICH, P., MANGENEY, A., GUIBOURG, S., and ROCHE, R. (1998), *Simulation of Water Waves Generated by a Potential Debris Avalanche in Montserrat*, *Lesser Antilles*, Geophys. Res. Lett. *25* (19), 3697–3700.

HUTTER, K., *Avalanche dynamics*, *a review*. In *Hydrology of Disasters* (ed. Singh, V. P.) (Kluwer Academic Publishers, Amsterdam 1996) pp. 317–394.

JIANG, L., and LEBLOND, P. (1992), *The Coupling of a Submarine Slide and the Surface Waves which it Generates*, J. Geophys. Res. *97* (12), 731–744.

JIANG, L., and LEBLOND, P. (1993), *Numerical Modeling of an Underwater Bingham Plastic Mudslide and the Waves which it Generates*, J. Geophys. Res. *98*, 304–317.

KULIKOV, E. A., RABINOVICH, A. B., THOMSON, R. E., and BORNHOLD, B. D. (1996), *The Landslide Tsunami of November 3, 1994, Skagway Harbor*, *Alaska*, J. of Geophysical Res. Oceans *101* (C3), 6609–6615.

MANGENEY, A., HEINRICH, PH., and ROCHE, R. (2000), *Analytical and Numerical Solution of Dam-break Problem for Application to Water Floods*, *Debris and Dense Snow Avalanches*, Pure appl. geophys. *157*, 1081–1096.

MIP (1981), *Mission d'Inspection Pluridisciplinaire sur le sinistre de Nice du 16 Octobre 1979*, Rapport final (unpublished report).

MULDER, T., SAVOYE, B., and SYVITSKI, J. P. (1997), *Numerical Modelling of a Mid-sized Gravity Flow: The 1979 Nice Turbidity Current (Dynamics, Processes, Sediment Budget and Seafloor Impact)*, Sedimentology *44*, 305–326.

NOREM, H., LOCAT, J., and SCHIELDROP, B. (1991), *An Approach to the Physics and the Modelling of Submarine Flowslides*, Mar. Geotechnol. *9*, 93–111.

PAUTOT, G. (1981), *Cadre morphologique de la Baie des Anges. Modèle d'instabilité de la pente continentale*, Oceanologica Acta *4*, 203–212.

PIPER, D. J. W., and SAVOYE, B. (1993), *Process of late Quaternary Turbidity Current Flow and Deposition on the Var Deep-sea Fan*, *Northwest Mediterranean Sea*, Sedimentology *40*, 557–582.

SABATIER, P. C., *Formation of waves by ground motion*. In *Encyclopedia of Fluid Mechanics* (Gulf Publishing Company P.O. Box 2608, Houston, Texas. 77001 1986), *17*, pp. 723–759.

(Received September 1, 1999, accepted March 15, 2000)